Quantum theory of nonlinear loop mirrors

K. J. Blow, Rodney Loudon,* and Simon J. D. Phoenix
BT Laboratories, Martlesham Heath, Ipswich IP5 7RE, Suffolk, United Kingdom
(Received 26 November 1991)

We formulate a continuous-mode quantum theory of nonlinear loop mirrors. We exploit the "conservation of squeezing" property at a beam splitter to provide a particularly simple description of the output noise spectra from such devices. We also derive a general condition for which one may obtain a squeezed vacuum from one of the output ports of the loop mirror.

PACS number(s): 42.50.Dv, 42.50.Rh, 42.79.Ta

I. INTRODUCTION

Four-wave-mixing processes provide effective mechanisms for the production of broadband squeezed light. The squeezing process occurs via the self-phase modulation associated with the Kerr nonlinearity, and it offers the important advantages of automatic phase matching and occurrence in isotropic materials, the Kerr effect being derived from a third-order nonlinear susceptibility. Since the original proposals of four-wave mixing [1,2], there have been detailed studies of the squeezing produced in propagation along optical fibers [3]. The earlier calculations of self-phase modulation used theories based on the discrete-mode quantization of the electromagnetic field, which was assumed to be confined within an optical cavity. Recently, we have developed a continuous-mode quantization scheme for the electromagnetic field [4], which is particularly appropriate for calculations of pulse propagation in long optical fibers where there is in reality no confining cavity. These methods have been used for calculations of the squeezing spectra produced by self-phase modulation in optical fibers [5]. We have shown that the Kerr-effect response time of the fiber material, although only of the order of femtoseconds for silica, is an important parameter in determining the dynamics of the squeezing process.

The self-phase modulation properties of optical fibers are put to effective practical use in the nonlinear Sagnac interferometer, or nonlinear fiber loop mirror, which is a particularly promising device for all-optical signal processing [6–8]. Shirasaki and Haus [9] pointed out that the device should also be useful for the observation of squeezed light produced by self-phase modulation, since in contrast to a simple length of optical fiber, it allows a low-intensity squeezed component of the light to be spatially separated from the surviving high-intensity pump. Recent experiments have demonstrated the significance of the nonlinear Sagnac interferometer for the production and detection of squeezed light [10,11].

We aim in the present paper to apply our previous calculations for self-phase modulation in optical fibers to the Sagnac interferometer. The previous theory is summarized and extended in Sec. II. We show that the squeezing spectrum of a square pulse can be expressed in analytic form in terms of two angles that describe the Kerr phase shift according to classical theory and the phase shift associated with the quantum-mechanical vacuum. The vacuum phase shift is ordinarily about five orders of magnitude smaller than the classical phase shift, and we provide simple expansions of the squeezing properties in powers of the vacuum phase shift. Similar results for the nonlinear Sagnac interferometer are presented in Sec. III, particularly for a single input beam. Results for arbitrary input pulses are derived and it is shown that the squeezing spectrum is simply related to that for ordinary fibers. Simple expansions of the squeezing properties are given for the case of a square input pulse. We also discuss the use of the "conservation of squeezing" property for a beam splitter [12] in the interpretation of these results and for the prediction of new properties of these nonlinear interferometers.

II. SELF-PHASE MODULATION

In this section we review and extend the theory of self-phase modulation given previously by us [5]. We evaluate the squeezing spectrum for a square pulse, obtaining both an exact analytic expression and an approximation valid for propagation in typical optical fibers. The square pulse is chosen because the nonlinear phase shift is constant across such a pulse and the degree of squeezing obtained is larger [5]. Furthermore, the mathematical expressions needed to describe the quantum propagation of a square pulse in a nondispersive nonlinear medium are easily obtainable in closed form. The theory of self-phase modulation used previously by us is expressed in terms of renormalized length and nonlinear parameters given by

$$L=\frac{n_0\omega_0 z}{c}\ , \tag{2.1}$$

$$\kappa=\frac{n_2\hbar\omega_0}{4\epsilon_0 n_0^3 c A}\ , \tag{2.2}$$

where the linear and the Kerr contributions form the nonlinear refractive index

$$n=n_0+\frac{n_2}{2n_0}|E|^2\ , \tag{2.3}$$

ω_0 is the central pulse frequency, z is the propagation distance, and A is the nonlinear effective cross section of the

fiber mode. The solution of the propagation equation for the continuum-mode photon destruction operator is

$$\hat{a}(L,t)=\exp\left[-i\kappa L\int_0^\infty d\tau\, g(\tau)\hat{a}^\dagger(0,t-\tau)\hat{a}(0,t-\tau)\right]\times\hat{a}(0,t)\ , \tag{2.4}$$

where $g(\tau)$ is a normalized function that describes the temporal response of the fiber material to the Kerr effect, and t is the time in the frame moving with the group velocity of the medium. The response time τ_0 in silica is of the order of 10^{-14} s (throughout this paper we shall assume a value of 5 fs for the response time) and the exact form of the response function is not important when the other time scales in the system are much longer than this. We shall write (2.4) in the equivalent form

$$\hat{a}_{\rm out}(t)=\hat{\Omega}(t)\hat{a}_{\rm in}(t)\ , \tag{2.5}$$

where $\hat{\Omega}(t)$ is the nonlinear propagator that takes the input operator $\hat{a}_{\rm in}$ to the output operator $\hat{a}_{\rm out}$. Throughout the present work we take the simple form

$$g(\tau)=\begin{cases}1/\tau_0, & \tau<\tau_0\\ 0, & \tau>\tau_0\ .\end{cases} \tag{2.6}$$

Then with the use of the normal-ordering theorem [4], the nonlinear propagator defined in (2.5) can be written in the form

$$\hat{\Omega}(t)=\ :\exp\left[(e^{-i\kappa L/\tau_0}-1)\times\int_0^{\tau_0}d\tau\,\hat{a}^\dagger(0,t-\tau)\hat{a}(0,t-\tau)\right]:\ , \tag{2.7}$$

where the colons denote normal ordering. The quantity Φ_v defined by

$$\Phi_v=\kappa L/\tau_0 \tag{2.8}$$

is the vacuum phase shift whose physical significance has been extensively discussed in Ref. [5]. If the expectation values of the operators in (2.4) show only negligible changes over the response time scale, then the nonlinear propagator reduces to

$$\hat{\Omega}(t)=\ :\exp[(e^{-i\Phi_v}-1)\tau_0\hat{a}_{\rm in}^\dagger(t)\hat{a}_{\rm in}(t)]: \tag{2.9}$$

to a very good approximation.

The above formalism has been used in Ref. [5] to calculate the squeezing spectrum that can be observed by measurements of the quadrature operator

$$\hat{X}_{\rm out}(t)=\hat{a}_{\rm out}(t)e^{-i\phi}+\hat{a}_{\rm out}^\dagger(t)e^{i\phi}\ , \tag{2.10}$$

selected by the phase ϕ of the local oscillator in homodyne detection. The resulting noise spectrum is

$$S(\omega,\phi)=\frac{1}{T}\int_{t_0-T/2}^{t_0+T/2}dt\int_{t_0-T/2}^{t_0+T/2}dt'V(t,t')e^{i\omega(t-t')}\ , \tag{2.11}$$

where we have written the two-time correlation function

$$V(t,t')=\langle\hat{X}_{\rm out}(t)\hat{X}_{\rm out}(t')\rangle-\langle\hat{X}_{\rm out}(t)\rangle\langle\hat{X}_{\rm out}(t')\rangle \tag{2.12}$$

and the explicit expression for an input coherent state $|\{\alpha(t)\}\rangle$ is

$$V(t,t')=\alpha(t)\alpha(t')\exp\{-2i\phi+G(\Phi_v)[|\alpha(t)|^2+|\alpha(t')|^2]\}\{\exp[-i\Phi_v\tau_0 g(t'-t)+|\alpha(t')|^2H_1(\Phi_v,t-t')]-1\}$$
$$+\alpha^*(t)\alpha(t')\exp[G^*(\Phi_v)|\alpha(t)|^2+G(\Phi_v)|\alpha(t')|^2]\{\exp[|\alpha(t')|^2H_2(\Phi_v,t-t')]-1\}+\text{c.c.}+\delta(t-t')\ . \tag{2.13}$$

The auxiliary functions in this expression, with the adoption of the response function (2.5), are given by

$$G(\Phi_v)=(e^{-i\Phi_v}-1)\tau_0\ ,$$
$$H_1(\Phi_v,s)=(e^{-i\Phi_v}-1)^2(\tau_0-|s|)\Theta(\tau_0-|s|)\ , \tag{2.14}$$
$$H_2(\Phi_v,s)=|e^{-i\Phi_v}-1|^2(\tau_0-|s|)\Theta(\tau_0-|s|)\ ,$$

where $\Theta(t)$ is the Heaviside unit step function. The variance (2.13) vanishes for $|t-t'|>\tau_0$, and the spectrum (2.11) is accordingly independent of ω for frequencies much smaller than 10^{14} Hz. We restrict attention to such frequencies, setting ω equal to zero in (2.11).

An important special case in which the integrations in (2.11) can be performed analytically is provided by the self-phase modulation of a coherent input state of constant flux $|\alpha(t)|^2$. We therefore put

$$\alpha(t)=|\alpha|e^{i\Phi_\alpha}\ , \tag{2.15}$$

where $|\alpha|$ is a constant that determines the number N of photons received by the detector in the integration time T according to

$$N=|\alpha|^2T\ . \tag{2.16}$$

Equivalently, one can think in terms of a square pulse of width T incident on the detector. The expectation value of (2.4) with the approximations discussed above for the input coherent state (2.15) is given by

$$\langle\hat{a}_{\rm out}(t)\rangle=\exp[i\Phi_\alpha+(e^{-i\Phi_v}-1)\tau_0|\alpha|^2]|\alpha|\ . \tag{2.17}$$

The normal-ordering factor $\exp(-i\Phi_v)-1$ arises from the commutation properties of the field operators, and it reduces to $-i\Phi_v$ if the operators are treated like classical amplitudes. In this case (2.17) reduces to

$$\langle\hat{a}_{\rm out}(t)\rangle=\exp(i\Phi_\alpha-i\Phi_c)|\alpha|\ , \tag{2.18}$$

where (2.8) has been used and the classical phase shift Φ_c is defined by

$$\Phi_c = \kappa L |\alpha|^2 . \tag{2.19}$$

The derivations that follow use the correct quantum-mechanical expectation values, including (2.17), but the results are conveniently expressed in terms of the phase shifts defined in (2.8) and (2.19).

It is straightforward to evaluate the noise spectrum (2.11) for the coherent state specified by (2.15) and the result is

$$S(0,\phi) = 1+2\,\mathrm{Re}\left[\exp\left[2i(\Phi_\alpha-\phi)+2(e^{-i\Phi_v}-1)\frac{\Phi_c}{\Phi_v}\right]\left[(e^{-i\Phi_v}+1)\frac{\exp[(e^{-i\Phi_v}-1)^2\Phi_c/\Phi_v]-1}{(e^{-i\Phi_v}-1)^2}-2\frac{\Phi_c}{\Phi_v}\right]\right]$$
$$+2\exp\left[-2(1-\cos\Phi_v)\frac{\Phi_c}{\Phi_v}\right]\left[\frac{\exp[2(1-\cos\Phi_v)\Phi_c/\Phi_v]-1}{1-\cos\Phi_v}-2\frac{\Phi_c}{\Phi_v}\right] . \tag{2.20}$$

It is seen that the noise is entirely controlled by the two phase shifts, and it is important to consider their magnitudes in greater detail. For a 1-W beam of 1.05 μm radiation $|\alpha|^2 = 5\times10^{18}$ s^{-1} and with the value of τ_0 given above, it follows from (2.8) and (2.19) that

$$\Phi_v \approx 4\times10^{-5}\Phi_c . \tag{2.21}$$

The parameters that occur in (2.1) and (2.2) are such that $\Phi_c \approx 4.5$ for a 1-km length of silica-based fiber. It follows that Φ_c can take values much larger than unity for practical values of the experimental parameters but that Φ_v is generally much smaller than unity.

It is instructive to expand the somewhat complicated expression (2.20) for the noise spectrum in powers of Φ_v, and the constant and linear terms give

$$S(0,\phi) = 1+2\Phi_c^2-\tfrac{4}{3}\Phi_c^3\Phi_v - \Phi_c(2\Phi_c+\Phi_v-\tfrac{8}{3}\Phi_c^2\Phi_v)\cos2\Theta - \Phi_c(2-5\Phi_c\Phi_v)\sin2\Theta , \tag{2.22}$$

where we have written

$$\Theta = \phi+\Phi_c-\Phi_\alpha . \tag{2.23}$$

This expression has the standard form of a squeezed-state variance and its main properties follow from well-known procedures [13]. The variance takes extremal values for phase angles that satisfy

$$\tan2\Theta = \frac{2-5\Phi_c\Phi_v}{2\Phi_c+\Phi_v-\frac{8}{3}\Phi_c^2\Phi_v} , \tag{2.24}$$

and the corresponding maximum and minimum variances are

$$S(0,\phi)_{\substack{\max\\\min}} = 1+2\Phi_c^2-\tfrac{4}{3}\Phi_c^3\Phi_v \pm 2\Phi_c(1+\Phi_c^2-4\Phi_c\Phi_v-\tfrac{8}{3}\Phi_c^3\Phi_v)^{1/2} , \tag{2.25}$$

where the subscripts max and min refer to the + and − signs in (2.25), respectively. The product of the extremal variances satisfies

$$S(0,\phi)_{\max}S(0,\phi)_{\min} = 1+\tfrac{40}{3}\Phi_c^3\Phi_v+\tfrac{16}{3}\Phi_c^5\Phi_v+\cdots . \tag{2.26}$$

The terms of higher order in Φ_v can, of course, affect the size of the variance but we have shown that the next terms, of order Φ_v^2, are negligible for the propagation distances considered here. Figure 1 compares the product of maximum and minimum variances obtained exactly from (2.20) with the approximation (2.26).

The terms that contain Φ_v in the above expressions can be neglected for propagation distances much shorter than 1 km, when (2.25) reduces to

$$S(0,\phi)_{\substack{\max\\\min}} \approx 1+2\Phi_c^2\pm2\Phi_c(1+\Phi_c^2)^{1/2} . \tag{2.27}$$

In the same approximation the product of the maximum and minimum variances in (2.26) has the unit value that characterizes a minimum uncertainty or ideal squeezed state. The minimum variance given by the approximate expression (2.27) can be made arbitrarily small by the choice of a sufficiently large Φ_c. However, the amount of

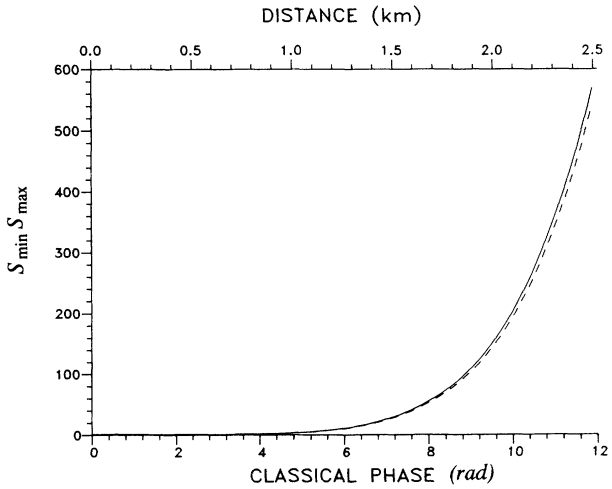

FIG. 1. Product of the minimum and maximum variances as a function of classical phase shift Φ_c and propagation distance. The solid line is the exact expression and the dashed curve is obtained by retaining only terms up to first order in the vacuum phase shift Φ_v. In this and subsequent figures, Φ_c is measured in radians.

squeezing that can be obtained in practice is limited by the growth of the terms in Φ_v as the propagation distance is increased. For classical phase shifts of around π the Φ_c^5 term begins to dominate and the propagated quantum state begins to deviate significantly from a minimum uncertainty state. For the numerical values of the various parameters assumed earlier in the section, a classical 2π phase shift occurs at a propagation distance of approximately 1.3 km. The variance product is approximately equal to 15 after this distance and the minimum uncertainty character of the light is well and truly lost. These effects are shown in more detail in Figs. 2 and 3 where the maximum and minimum variances are plotted as functions of the classical phase shift and propagation distance from the exact expression (2.20), with the $\Phi_v=0$ limits from (2.27) shown by the dashed curves. It is important to remember that the curves given as functions of the classical phase shift are universal curves for a given fiber response time. The contribution to the maximum variance from the vacuum phase shift is small, as can be seen in Fig. 2, and the approximation of setting Φ_v equal to zero is valid in this case. For the minimum variance, however, the inclusion of the vacuum phase shift has a significant effect. It is seen, in Fig. 3, that the terms in Φ_v become important at about a classical phase shift of π and the minimum variance begins to increase for increasing classical phase shift. However, substantial degrees of squeezing still survive for classical phase shifts up to about 3π (propagation distances of about 2 km for the above parameters). Qualitatively similar behavior of the variance has been calculated and illustrated by Tanas, Miranowicz, and Kielich [14]. Figure 4 shows the ways in which the detection phase angles for maximum and minimum variances depend on the propagation distance. It is important to note that the photon number variance remains Poissonian throughout the propagation. The degradation of the squeezing for higher classical phase

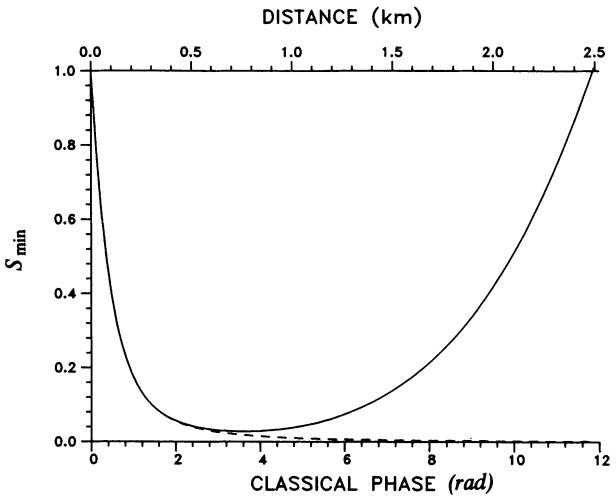

FIG. 3. Minimum variance as a function of classical phase shift and propagation distance. The solid curve is the exact expression and the dashed curve is obtained by setting the vacuum phase shift to zero.

shifts is associated with the production of crescent-shaped quasiprobability distributions in single-mode theories [14–16]. Of course, the nonlinear coefficient considered here is not sufficient to take us into the regime where we might observe the production of superpositions of coherent states [17]. However, the excess noise for classical phase shifts of a few π, shown in Fig. 3, may be partly responsible for the excess noise observed in recent quantum soliton experiments [10].

The solution for self-phase modulation presented above is derived from a noncanonical theory. The noncanonical nature of the above theory arises because we have included a finite (nonzero), albeit extremely rapid, response time. This leads to nonlinear absorption, which intro-

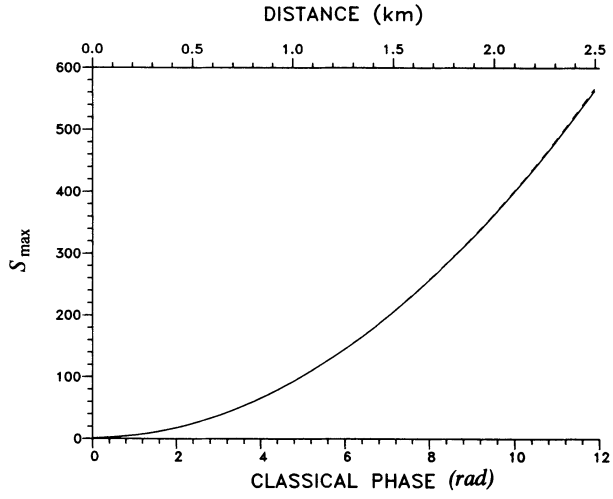

FIG. 2. Maximum variance as a function of classical phase shift and propagation distance. The solid curve is the exact expression and the dashed curve is obtained by setting the vacuum phase shift to zero.

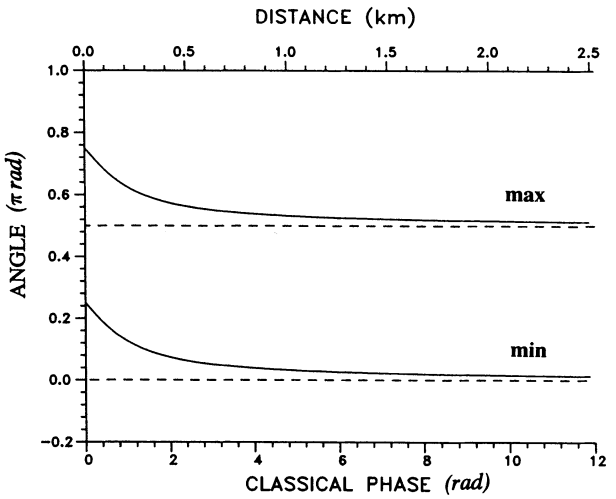

FIG. 4. Detection phase angle Θ in units of π for maximum and minimum variances as a function of classical phase shift and propagation distance.

duces an extra noise source into the propagation equation. Our argument is essentially that because the physical response time is so rapid, this noise source is negligible and will not have a significant effect on the propagation of the quantum noise, provided that the classical nonlinear absorption is also negligible. As a consequence of the absence of this extra noise source, the commutation relation between the field creation and annihilation operators is not conserved under propagation and is equal to a δ function plus a correction term. This correction, which must be included in the squeezing spectrum to account for this noncanonical approach, is first order in Φ_v [5] and cannot obviously be neglected in (2.25). However, plots of $S_{\min}$ with and without this additional contribution are almost indistinguishable up to classical phase shifts of around 4π. This is because at small distances the correction term is much smaller than the classical contribution and at large distances it is much smaller than the dominant quantum contribution, which is proportional to $\Phi_c^5\Phi_v$. At these classical phase shifts we would expect Raman effects to become significant and the theory we have developed here and elsewhere [5] begins to break down. The Raman term can be modeled by an extension to the response function [5] and this is the basis of a recent approach [18]. Up to this phase shift, however, the extra noise contribution can be neglected in the squeezing spectrum.

III. NONLINEAR SAGNAC INTERFEROMETER

A. Conservation of squeezing

In this section we will be concerned with obtaining an understanding of the operation of the nonlinear Sagnac interferometer. Specifically, we shall have an eye on applications that involve the nonlinear loop mirror [6], which is a particular manifestation of the Sagnac interferometer. We shall find it convenient to generalize the analysis slightly to include nonlinear Mach-Zehnder interferometers. By modeling the loop mirror as an arrangement of beam splitters in the Mach-Zehnder configuration, many of the more important properties can be readily deduced by a judicious combination of the linear operation of the device and the input-output relations for the noise spectra. We shall be interested, primarily, in two quantities: the output photon fluxes from the arms, and the output noise spectra as defined by (2.10)–(2.12). Although the output flux is calculated in the usual way by tracking all the operators through the various input-output stages of the device, the output noise spectra can be inferred rather more readily, as we shall show below. This allows one to develop a powerful intuition concerning the potential squeezing properties of nonlinear interferometers and the techniques we present here can easily be extended to the case where the interferometer has different media in its internal arms.

The key ingredients of the nonlinear interferometer, in all its various guises, are the beam splitters and couplers that form the input and output ports of the device. One common approach taken in treating beam splitters with quantum inputs is to use the standard input-output relations for the operators that describe the input and output quantum fields. This approach is useful for quantities such as the photon flux, but it quickly becomes unwieldy when the output noise properties are required. It is therefore convenient, and physically more intuitive, to make use of an earlier result of Fearn and Loudon [12], which describes a conservation of squeezing property at a linear lossless beam splitter. This result relates the noise spectra at the outputs of a linear lossless beam splitter to the noise spectra at the inputs, thus forming an input-output relation for the noise spectra.

With the above remarks in mind, we first consider the input-output properties of a single beam splitter. The properties of beam splitters and couplers with respect to quantum inputs have been discussed by many authors. A comprehensive discussion, highlighting many new features (especially in the lossy case) and with references to earlier work, has recently been given by Lai, Buzek, and Knight [19]. We consider a single beam splitter, as shown schematically in Fig. 5, together with the notation for the input and output operators. We assume that the reflection and transmission coefficients p and q, respectively, are independent of frequency and satisfy the usual unitarity requirements

$$|p|^2+|q|^2=1, \quad p^*q+pq^*=0 . \tag{3.1}$$

Without loss of generality we shall assume p to be real so that $q=i|q|$. The conservation of squeezing property of the beam splitter can conveniently be expressed by the formulas [12]

$$\begin{aligned} S_3(\phi)&=|p|^2S_2(\phi)+|q|^2S_1(\phi-\pi/2) , \\ S_4(\phi)&=|q|^2S_2(\phi-\pi/2)+|p|^2S_1(\phi) , \end{aligned} \tag{3.2}$$

where we have used the notation $S_j(\phi)$ to denote the noise spectrum in arm j. The spectrum is defined in Eqs. (2.10)–(2.14). As we have shown above, for modest classical phase shifts and an input coherent state, the output from a nonlinear $\chi^{(3)}$ medium such as an optical fiber is a minimum uncertainty ideal squeezed state. It is instructive, therefore, to consider the result (3.2) in a single mode and with input ideal squeezed states. The maximum degree of squeezing in a given output is obtained when the orientation of the error ellipses for the two in-

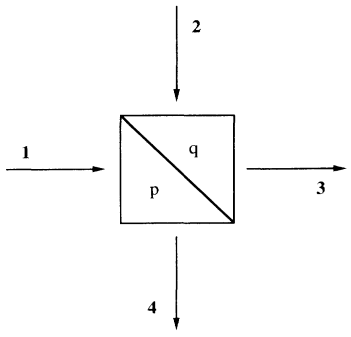

FIG. 5. Schematic of a single beam splitter with reflection and transmission coefficients p and q showing the notation for the input and output operators.

puts are orthogonal. Let us suppose that this is indeed the case and that the inputs have squeezing parameters η_1 and η_2 such that $\eta_1 > \eta_2$ and input 1 is the more highly squeezed. We can write

$$S_1(\phi)=\exp(-2\eta_1),\quad S_1(\phi-\pi/2)=\exp(2\eta_1)\ ,$$
$$S_2(\phi)=\exp(2\eta_2),\quad S_2(\phi-\pi/2)=\exp(-2\eta_2)\ , \tag{3.3}$$

so that from (3.2) we have

$$S_3(\phi)=|p|^2\exp(2\eta_2)+|q|^2\exp(2\eta_1)\ ,$$
$$S_4(\phi)=|p|^2\exp(-2\eta_1)+|q|^2\exp(-2\eta_2)\ . \tag{3.4}$$

Application of the unitarity condition (3.1) to Eq. (3.2) enables one to write the output noise spectra in arms 3 and 4 of the beam splitter as

$$S_3(\phi-\pi/2)=S_1(\phi)+|p|^2[S_2(\phi-\pi/2)-S_1(\phi)]\ ,$$
$$S_4(\phi)=S_1(\phi)+|q|^2[S_2(\phi-\pi/2)-S_1(\phi)]\ . \tag{3.5}$$

By supposition we have that the maximum squeezing in arm 1 is greater than the maximum squeezing in arm 2; thus for the inputs considered above we have

$$S_3(\phi-\pi/2)=S_1(\phi)_{\min}+|p|^2[\exp(-2\eta_2)-\exp(-2\eta_1)]$$
$$\geq S_1(\phi)_{\min}\ ,$$
$$S_4(\phi)=S_1(\phi)_{\min}+|q|^2[\exp(-2\eta_2)-\exp(-2\eta_1)] \tag{3.6}$$
$$\geq S_1(\phi)_{\min}\ .$$

A similar application of the unitarity condition (3.1) to Eqs. (3.2) leads to the following inequalities between the minimum variances obtainable from the output ports:

$$S_1(\phi)_{\min}\leq S_{3,4}(\phi)_{\min}\leq S_2(\phi)_{\min}\ . \tag{3.7}$$

Consequently, one cannot obtain a higher degree of squeezing in either of the output arms than is present in either of the input arms alone. The equalities in the above expression hold if $\eta_1=\eta_2$ and the squeezing in both arms is of equal strength.

The above analysis is valid for two orthogonally squeezed inputs. It is instructive to consider the case of two ideal squeezed states with arbitrary squeezing orientations as inputs to the beam splitter. The detection angle is fixed so that it is aligned with the direction of maximum squeezing in input arm 1. The output spectrum in arm 4 is now a function of the angle θ between the orientation of the error ellipses and is given by

$$S_4(\theta)=\exp(-2\eta_1)$$
$$+|q|^2\{[\exp(-2\eta_2)-\exp(-2\eta_1)]\sin^2\theta$$
$$+[\exp(2\eta_2)-\exp(-2\eta_1)]\cos^2\theta\}\ . \tag{3.8}$$

The term in $\cos^2\theta$ is always positive and reduces the degree of squeezing. This is because of the positive exponential term that arises from the unsqueezed quadrature of the input in arm 2. This term can be so large that the squeezing in arm 4 is completely destroyed. As the squeezing in arm 2 is increased, the range of values of θ for which squeezing is observed in arm 4 is reduced (for fixed reflection and transmission coefficients).

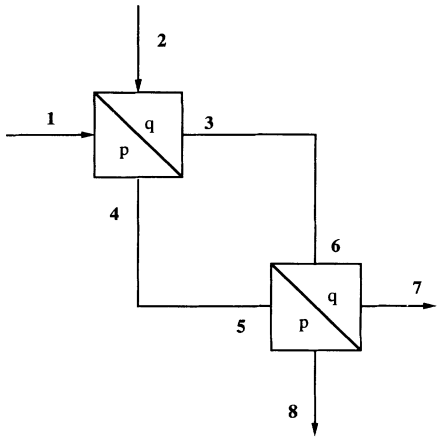

FIG. 6. Schematic of a Mach-Zehnder interferometer showing the labeling of the input, output, and internal arms of the device.

We are now in a position to understand some of the important noise properties of the nonlinear loop mirror, which can be modeled as the Mach-Zehnder arrangement shown schematically in Fig. 6. In the Mach-Zehnder configuration of Fig. 6, the function of the first beam splitter is to allow unequal intensities into the internal arms so that differential classical phase shifts are produced in the nonlinear media, and also to produce a $\pi/2$ phase shift upon transmission. The nonlinear media produce squeezing via the self-phase modulation process and the maximum degree of squeezing obtainable from output arms 7 or 8 cannot be greater than the maximum degree of squeezing at inputs 5 or 6. In general it will be less because the differential phase shifts in the internal arms due to the nonlinear propagation will ensure that the two input squeezed states at 5 and 6 are not orthogonally squeezed. In fact, as we have demonstrated above, there are some values of the classical phase shift that give a nonsqueezed output state even though the individual

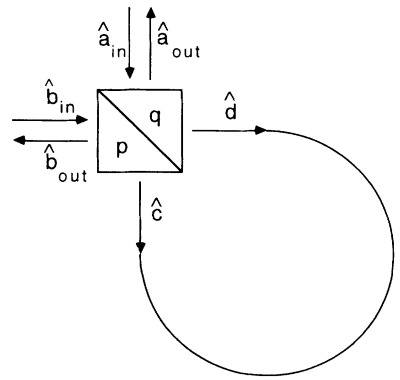

FIG. 7. Schematic of the fiber loop mirror showing the notation for the operators at the input, output, and internal arms of the device.

states in the internal arms of the device are squeezed. We discuss a situation where this effect is important in Sec. III C. It goes without saying that to achieve orthogonally squeezed inputs at 5 and 6 requires careful adjustment of the initial amplitudes at the input arms 1 and 2.

B. Vacuum input to arm 2

We now consider the operation of the nonlinear loop mirror, shown schematically in Fig. 7. The loop mirror is basically a "folded" Mach-Zehnder interferometer and the results of Sec. III A can be readily applied. The input modes $\hat{a}_{\rm in}$ and $\hat{b}_{\rm in}$ are equivalent to arms 1 and 2, respectively, in the Mach-Zehnder configuration of Fig. 6 and the loop mirror output modes $\hat{a}_{\rm out}$ and $\hat{b}_{\rm out}$ correspond to arms 7 and 8, respectively. With an input coherent state $|\alpha(t)\rangle$ to the $\hat{a}_{\rm in}(t)$ mode and a vacuum input to the $\hat{b}_{\rm in}(t)$ mode, the output flux in the $\hat{b}_{\rm out}(t)$ mode can easily be calculated from the expression

$$\hat{b}_{\rm out}(t)=q\hat{\Omega}_c(t)\hat{c}(t)+p\hat{\Omega}_d(t)\hat{d}(t)\ , \tag{3.9}$$

where the $\hat{\Omega}$ operators are defined by (2.5) with the $\hat{a}$ operators replaced by $\hat{c}$ or $\hat{d}$ operators. The output flux is then given by

$$\langle\hat{b}^\dagger_{\rm out}(t)\hat{b}_{\rm out}(t)\rangle=|\alpha(t)|^2(\,|p|^4+|q|^4-|pq|^2\exp\{[\,|q|^2G^*(\Phi_v)+|p|^2G(\Phi_v)]|\alpha(t)|^2\}$$
$$-|pq|^2\exp\{[\,|p|^2G^*(\Phi_v)+|q|^2G(\Phi_v)]|\alpha(t)|^2]\}\,)\ . \tag{3.10}$$

This gives the usual result

$$\langle\hat{b}^\dagger_{\rm out}(t)\hat{b}_{\rm out}(t)\rangle=(|q|^2-|p|^2)^2|\alpha(t)|^2\quad(G=0)\ , \tag{3.11}$$

when the Kerr coefficient κ is set equal to zero.

The output flux (3.10) is readily evaluated for the constant input pulse defined in (2.15), and its expansion in powers of the vacuum phase shift is

$$\langle\hat{b}^\dagger_{\rm out}(t)\hat{b}_{\rm out}(t)\rangle$$
$$=|\alpha|^2\{\,|p|^4+|q|^4-2|pq|^2\cos[(|q|^2-|p|^2)\Phi_c\,]$$
$$\times(1-\tfrac{1}{2}\Phi_c\Phi_v)\}\ . \tag{3.12}$$

The noise spectrum, or variance, achieves its fully developed form only for integration times at least as long as the material response time τ_0. The material response time is typically much shorter than the detector resolving time, and experiments cannot in practice be carried out on the time scale of τ_0. However, the number of photons received by the detector in the period τ_0, given from (2.8), (2.19), and (3.12) as

$$N_{\rm min}=\frac{\Phi_c}{\Phi_v}\{\,|p|^4+|q|^4-2|pq|^2\cos[(|q|^2-|p|^2)\Phi_c\,]$$
$$\times(1-\tfrac{1}{2}\Phi_c\Phi_v)\}\ , \tag{3.13}$$

provides a measure of the minimum input to the detector needed to detect the presence of squeezing.

The output squeezing spectrum is now easily calculated from the conservation of squeezing property. The first passage through the coupler produces the counterpropagating coherent states $|p\alpha(t)\rangle$ and $|q\alpha(t)\rangle$. These states propagate through the nonlinear medium and are squeezed by their interaction with this medium as described in Sec. II. These states are then recombined at the second passage through the coupler to produce an output noise spectrum in the $\hat{b}_{\rm out}(t)$ mode

$$S_b(\phi)=|p|^2S_d(\phi)+|q|^2S_c(\phi-\pi/2)\ . \tag{3.14}$$

The noise spectra S_d and S_c are given by expressions (2.10)–(2.14) but with $\alpha(t)$ replaced by $p\alpha(t)$ and $q\alpha(t)$, respectively. Thus we have the situation where two squeezed states, with different squeezing parameters, phases, and orientations are incident on a beam splitter or coupler. Clearly, from our previous discussion, the output from mode $\hat{b}_{\rm out}(t)$ may be squeezed. Apart from the trivial $\pi/2$ phase shift, the differences between the two incident squeezed states occur solely because of the differential classical phase shifts experienced by the counterpropagating pulses, which in turn are due to the input amplitudes and the splitting ratio at the first beam splitter or coupler. The noise spectrum (3.14) is simply the weighted sum of the noise spectra from two single pieces of fiber. There is nothing about the loop mirror configuration *per se* that is intrinsic to the production of squeezing; the nonclassical properties occur because of independent propagation in single pieces of fiber.

An important special case occurs when the loop mirror is perfectly balanced so that $|p|^2=|q|^2=\frac{1}{2}$. This case has been examined previously by Shirasaki and Haus [9] and is of direct relevance to squeezing experiments [11]. Here we shall reexamine this situation and highlight some additional features that emerge. The principal property of the balanced device, as shown by Shirasaki and Haus [9], is to allow separation of the squeezed pump wave emerging from one output port from the pulse of squeezed vacuum emerging from the other. This is important in squeezing experiments if problems of detector saturation are to be avoided. The separation of the "pump" from the "vacuum signal" is entirely a linear classical property of the device and it occurs regardless of the nature of the input light [20]. In the quantum-mechanical case, for modest classical phase shifts in the internal arms, a squeezed vacuum emerges from the vacuum output. There is thus a small quantum correction to be made in the output intensities of the two arms. We shall evaluate this correction below.

The first passage through the coupler splits the input light equally in both arms, giving rise to identical classical phase shifts in the counterpropagating fields. The coupler also generates a $\pi/2$ phase difference between these fields so that the fields entering the coupler for the second time are orthogonally squeezed. As we have dis-

cussed above, in the limit of a small classical phase shift, the output fields from the loop mirror will then be ideal squeezed states. The conservation of the squeezing property ensures that the squeezing in the output arms cannot be greater than the maximum squeezing generated in the internal arms of the device by the separate counterpropagating fields. Indeed, for the case of perfect balancing, it is evident from (3.2) that the noise spectra of the outputs are *identical* to the noise spectra of the counterpropagating fields. The noise spectrum for the output mode $\hat{b}_{\text{out}}(t)$ from which the squeezed vacuum emerges is therefore *identical* to the noise spectrum obtained from the output of a single piece of fiber, provided we make the replacement $\alpha \rightarrow \alpha/\sqrt{2}$. Thus we can observe precisely the same squeezing from the output of a loop mirror as from the output of a fiber provided that the input intensity to the loop mirror is twice the input intensity to the single piece of fiber.

In Fig. 8 we plot the variation in the minimum noise spectrum as a function of the coupler coefficient for an incident square pulse of intensity 1 W. Figure 8(a) is for a 200-m length loop mirror and Fig. 8(b) is for a loop mirror length of 1 km. It can be seen from these curves that as the power-length product is increased, the coupling ratio required to observe squeezing in the output arm must be more carefully controlled. This is because the differential classical phase shift in the internal arms varies more rapidly with the coupler coefficient for higher input intensities at a given length. This, however, does not appear to lead to as stringent a requirement on the coupling ratio as does the necessity of avoiding detector saturation. In fact, it may be more advantageous to use lower powers in the loop so that significant squeezing can still be observed over a wider range of coupler ratios about the 50:50 point. It is also interesting to note that although the loop requires *twice* the input intensity to achieve precisely the same output noise spectrum as a single piece of fiber, the minimum noise shows little variation around 700 m (approximately π classical phase shift), as shown in Fig. 3. Thus the minimum noise at $|p|^2=\frac{1}{2}$ and $|p|^2=1$ for a 1-km loop length is approximately equal. This behavior can be seen in Fig. 8(b). This is not the case, however, for the 200-m loop length as the minimum noise in this region is a sharply varying function of the classical phase shift. Thus in Fig. 8(a) we see that the minimum noise is lower at $|p|^2=1$ than at $|p|^2=\frac{1}{2}$.

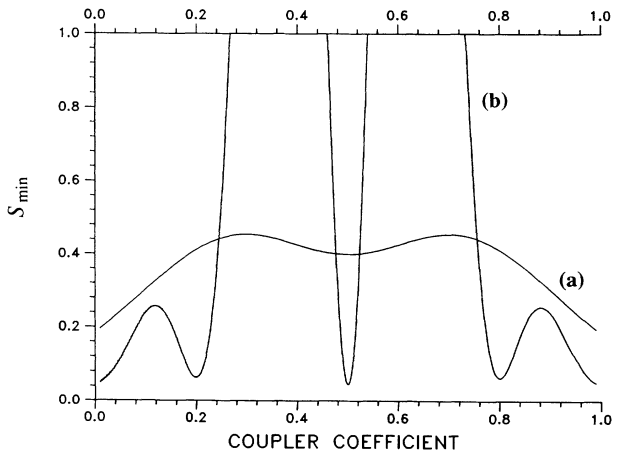

FIG. 8. Minimum variance in the output mode $\hat{b}_{\text{out}}$ as a function of the coupler coefficient for the loop. We have assumed a coherent input to the $\hat{a}_{\text{in}}$ mode of the interferometer and a vacuum input to the $\hat{b}_{\text{in}}$ mode. Curve (*a*) is for a loop length of 200 m. Curve (*b*) is for a loop length of 1 km.

For the square pulse excitation of (2.15) the minimum photon number required to observe the effects of squeezing can be expanded in powers of the vacuum phase shift and is, from (3.13), given by

$$N_{\text{min}}=\tfrac{1}{4}\Phi_c^2 , \tag{3.15}$$

and the minimum variance from (2.25) is (remembering that for the balanced loop mirror we must replace Φ_c with $\Phi_c/2$) given by

$$S(0,\phi)_{\text{min}}=1+\tfrac{1}{2}\Phi_c^2-\tfrac{1}{6}\Phi_c^3\Phi_v-\Phi_c(1+\tfrac{1}{4}\Phi_c^2-2\Phi_c\Phi_v-\tfrac{1}{3}\Phi_c^3\Phi_v)^{1/2} . \tag{3.16}$$

In the limit of $\Phi_c \ll 1$, corresponding to a propagation distance of less than 100 m or so, the variance reduces to

$$S(0,\phi)\approx 1-\Phi_c \quad (\Phi_c \ll 1) . \tag{3.17}$$

It is seen from (3.15) and (3.17) that the photon number in this case is of a higher order in Φ_c than the reduction of the variance below its vacuum magnitude of unity. The photon number is therefore smaller than this measure of the squeezing by a factor of Φ_c. Expressions identical to (3.15) and (3.17), to the given orders in Φ_c, are found for the mean photon number and quadrature variance of a discrete mode of the radiation field in a state consisting of a superposition of the vacuum $|0\rangle$ and the number state $|2\rangle$ with the expansion coefficients given by

$$|\psi\rangle=|0\rangle+\frac{\Phi_c}{\sqrt{8}}|2\rangle . \tag{3.18}$$

The squeezing produced by such superposition states has been extensively discussed by Wodkiewicz *et al.* [21].

C. General cancellation condition

As we have demonstrated above, the principal significance of using a balanced nonlinear loop mirror for squeezing experiments is the ability to produce a squeezed vacuum from one of the output ports. It is simply the linear properties of the device that yield the zero displacement, and it is the nonlinear propagation that generates the squeezing. There is, in linear operation, an alternative configuration of the loop mirror and its inputs that produces a vacuum in one of the output arms. The expectation, therefore, is that the nonlinear propagation changes the quantum noise properties of this vacuum state so that the state emerging from this port can be a squeezed vacuum. The balanced loop mirror considered earlier will be shown to be a special case of this more general configuration.

Consider the Mach-Zehnder configuration of the loop mirror as shown in Fig. 6. We initially suppose that the device is operated in the linear regime and that the inputs to arms 1 and 2 are the coherent states $|\alpha\rangle$ and $|\beta\rangle$, respectively. We shall consider only the case where the two beam splitters have identical properties, although the extension to different beam splitters is not difficult. The output coherent-state amplitude γ_{out} from arm 8 is given by

$$\gamma_{\text{out}}=(|p|^2-|q|^2)|\alpha|\exp(i\Phi_\alpha) +2|pq|\,|\beta|\exp[i(\Phi_\beta+\pi/2)]\,, \tag{3.19}$$

where $\Phi_{\alpha(\beta)}$ is the phase of the coherent state $|\alpha(\beta)\rangle$. The condition for achieving a vacuum output from arm 8 is clearly $\gamma_{\text{out}}=0$. This can be achieved if $|\alpha\rangle$ and $|\beta\rangle$ are $\pi/2$ out of phase and if we arrange the input intensities so that

$$|\beta|=\frac{|p|^2-|q|^2}{2|pq|}|\alpha|\,. \tag{3.20}$$

Condition (3.20) ensures that in linear operation the output from arm 8 is the vacuum. For a perfectly balanced Mach-Zehnder configuration, condition (3.20) can only be satisfied if $|\beta|=0$, which is the condition discussed in Sec. III B.

Let us now consider the situation where the nonlinearity is present in the internal arms. The output coherent states from the first beam splitter are given by

$$|\mu_3\rangle=\left|\frac{|\alpha|}{2|q|}\exp(i\pi/2)\right\rangle\,, \qquad |\mu_4\rangle=\left|\frac{|\alpha|}{2|p|}\right\rangle\,, \tag{3.21}$$

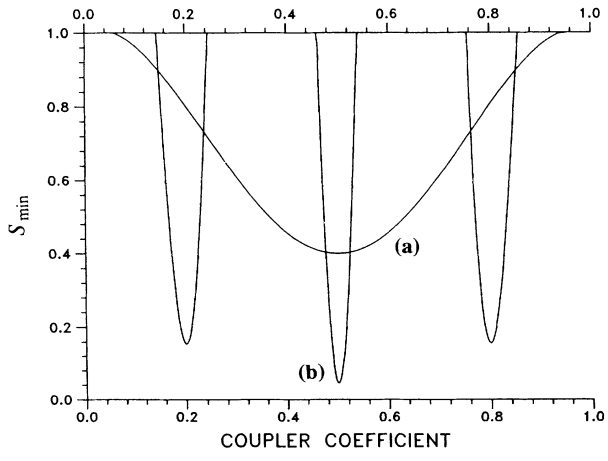

FIG. 9. Minimum variance in arm 8 as a function of the beam splitter coefficient for the Mach-Zehnder configuration. The device is assumed to be operating such that in the linear regime the output field in arm 8 is the vacuum and the sum of the input intensities is constant. Curve (*a*) is for an internal arm length of 200 m and curve (*b*) is for an internal arm length of 1 km.

where the subscripts denote the internal arms, as shown in Fig. 6, and we have used (3.20) and the unitarity condition (3.1) to obtain (3.21). We have also assumed, without loss of generality, that $\Phi_\alpha=0$. We note that there are unequal intensities propagating in the internal arms so that there is a differential phase shift $\delta\Phi_c$ determined approximately by

$$\delta\Phi_c=\tfrac{1}{4}\Phi_c^\alpha\left[\frac{1}{|q|^2}-\frac{1}{|p|^2}\right]\,, \tag{3.22}$$

where Φ_c^α is the classical phase shift experienced by the coherent state $|\alpha\rangle$ in a single piece of fiber. The two squeezed states incident upon the second beam splitter are not, in general, orthogonally squeezed. However, a squeezed vacuum still emerges from output arm 8 for certain values of the differential phase shift (3.22). The noise spectra can easily be determined by application of the conservation of squeezing property at the second beam splitter. In Fig. 9 we show the minimum squeezing from output arm 8 as a function of the beam splitter coefficient when the cancellation condition (3.20) is employed, subject to a constant total flux to the input arms 1 and 2 (that is, $|\alpha|^2+|\beta|^2=N=\text{const}$). The input pulses are taken to be square with a peak power of 1 W. Figure 9(a) is for a 200-m loop length and Fig. 9(b) is for a loop length of 1 km. The effect on the output squeezing of the differential classical phase shift in the internal arms can clearly be seen. The minima of the curve correspond to the inputs at arms 5 and 6 being orthogonally squeezed so that the differential classical phase shift at these points is a multiple of π. This requirement, together with the cancellation condition (3.20), implies that the minimum noise occurs at coupler coefficients such that

$$|p|^2_{\min}=\tfrac{1}{2}(1+m\pi/\Phi_c^N),\quad m=\ldots,-2,-1,0,1,2,\ldots, \tag{3.23}$$

where Φ_c^N is the classical phase shift experienced by a pulse with flux N in a single piece of fiber of a given length. For a 1-km length of fiber this quantity is approximately 4.5, so that (3.23) gives 3 minima occurring at $|p|^2_{\min}\approx 0.2, 0.5, 0.8$. This is in agreement with the exact curve shown in Fig. 9(b). There is only one minimum for curve 9(a) because $\Phi_c^N=0.9$ and this value is insufficient to give other minima in the physical range of coupler values $0\le|p|^2\le 1$.

IV. CONCLUSIONS

The potential of the nonlinear loop mirror for all-optical processing is now well established [6–8]. The recent developments of Haus and co-workers have also demonstrated the significance of the nonlinear loop mirror for the production and detection of squeezed light [9,11]. In this paper we have developed and extended our previous treatment of self-phase modulation in optical fibers [5] to investigate the regimes in which minimum uncertainty squeezing is obtained. We have applied this theory, together with the conservation of squeezing property at a beam splitter [12], to provide a particularly sim-

ple formulation of the noise properties of loop mirrors. This technique allows one to develop a powerful intuition concerning the squeezing properties of nonlinear interferometers. Furthermore, using this technique, one can readily analyze the situation with concatenated interferometers, and their input-output noise properties can quite trivially be obtained. Such devices have recently been studied in connection with using squeezed light in a fiber gyroscope [22].

The important property of the interferometer in balanced operation is the separation of the intense pump wave from the squeezed vacuum. We have presented a generalization of the balanced configuration that will also achieve this goal. This condition may well prove to be useful in future experiments involving nonlinear interferometers.

ACKNOWLEDGMENTS

We would like to thank S. M. Barnett, B. Huttner, A. J. Poustie, and P. D. Townsend for useful discussions concerning nonlinear propagation and the properties of interferometers.

*Permanent address: Physics Department, Essex University, Colchester CO4 3SQ, Essex, United Kingdom.

[1] H. P. Yuen and J. H. Shapiro, Opt. Lett. **4**, 334 (1979).
[2] R. Tanas and S. Kielich, Opt. Commun. **45**, 351 (1983).
[3] G. J. Milburn, M. D. Levenson, R. M. Shelby, S. H. Perlmutter, R. G. DeVoe, and D. F. Walls, J. Opt. Soc. Am. B **4**, 1476 (1987).
[4] K. J. Blow, R. Loudon, S. J. D. Phoenix, and T. J. Shepherd, Phys. Rev. A **42**, 4102 (1990).
[5] K. J. Blow, R. Loudon, and S. J. D. Phoenix, J. Opt. Am. B **8**, 1750 (1991).
[6] N. J. Doran and D. Wood, Opt. Lett. **13**, 56 (1988).
[7] K. J. Blow, N. J. Doran, and B. K. Nayar, Opt. Lett. **14**, 754 (1989).
[8] B. K. Nayar, K. J. Blow, and N. J. Doran, Opt. Comput. Proc. **1**, 81 (1991).
[9] M. Shirasaki and H. A. Haus, J. Opt. Soc. Am. B **7**, 30 (1990).
[10] M. Rosenbluh and R. M. Shelby, Phys. Rev. Lett. **66**, 153 (1991).
[11] K. Bergman and H. A. Haus, Opt. Lett. **16**, 663 (1991).
[12] H. Fearn and R. Loudon, Opt. Commun. **64**, 485 (1987).
[13] R. Loudon, Opt. Commun. **70**, 109 (1989).
[14] R. Tanas, A. Miranowicz, and S. Kielich, Phys. Rev. A **43**, 4014 (1991).
[15] M. Kitagawa and Y. Yamamoto, Phys. Rev. A **34**, 3974 (1986).
[16] A. Miranowicz, R. Tanas, and S. Kielich, Quantum Opt. **2**, 253 (1990).
[17] G. J. Milburn, Phys. Rev. A **33**, 674 (1986).
[18] S. J. Carter and P. D. Drummond, Phys. Rev. Lett. **67**, 3757 (1991).
[19] W. K. Lai, V. Buzek, and P. L. Knight, Phys. Rev. A **43**, 6323 (1991).
[20] D. B. Mortimore, IEEE J. Lightwave Technol. **6**, 1217 (1988).
[21] K. Wodkiewicz, P. L. Knight, S. M. Buckle, and S. M. Barnett, Phys. Rev. A **35**, 2567 (1987).
[22] H. A. Haus, K. Bergman, and Y. Lai, J. Opt. Soc. Am. B **8**, 1952 (1991).